

University of Groningen

Time-dependent density functional theory/discrete reaction field spectra of open shell systems

van Duijnen, Piet Th.; Greene, Shannon N.; Richards, Nigel G. J.

Published in:
Journal of Chemical Physics

DOI:
[10.1063/1.2751164](https://doi.org/10.1063/1.2751164)

IMPORTANT NOTE: You are advised to consult the publisher's version (publisher's PDF) if you wish to cite from it. Please check the document version below.

Document Version
Publisher's PDF, also known as Version of record

Publication date:
2007

[Link to publication in University of Groningen/UMCG research database](#)

Citation for published version (APA):

van Duijnen, P. T., Greene, S. N., & Richards, N. G. J. (2007). Time-dependent density functional theory/discrete reaction field spectra of open shell systems: The visual spectrum of [Fe-III(PyPepS)(2)](-) in aqueous solution. *Journal of Chemical Physics*, 127(4), [045105]. <https://doi.org/10.1063/1.2751164>

Copyright

Other than for strictly personal use, it is not permitted to download or to forward/distribute the text or part of it without the consent of the author(s) and/or copyright holder(s), unless the work is under an open content license (like Creative Commons).

The publication may also be distributed here under the terms of Article 25fa of the Dutch Copyright Act, indicated by the "Taverne" license. More information can be found on the University of Groningen website: <https://www.rug.nl/library/open-access/self-archiving-pure/taverne-amendment>.

Take-down policy

If you believe that this document breaches copyright please contact us providing details, and we will remove access to the work immediately and investigate your claim.

Downloaded from the University of Groningen/UMCG research database (Pure): <http://www.rug.nl/research/portal>. For technical reasons the number of authors shown on this cover page is limited to 10 maximum.

Time-dependent density functional theory/discrete reaction field spectra of open shell systems: The visual spectrum of $[\text{Fe}^{\text{III}}(\text{PyPepS})_2]$ in aqueous solution

Piet Th. van Duijnen, Shannon N. Greene, and Nigel G. J. Richards

Citation: [The Journal of Chemical Physics](#) **127**, 045105 (2007); doi: 10.1063/1.2751164

View online: <https://doi.org/10.1063/1.2751164>

View Table of Contents: <http://aip.scitation.org/toc/jcp/127/4>

Published by the [American Institute of Physics](#)

Articles you may be interested in

[Density-functional thermochemistry. III. The role of exact exchange](#)

[The Journal of Chemical Physics](#) **98**, 5648 (1993); 10.1063/1.464913

PHYSICS TODAY

WHITEPAPERS

ADVANCED LIGHT CURE ADHESIVES

Take a closer look at what these environmentally friendly adhesive systems can do

READ NOW

PRESENTED BY



Time-dependent density functional theory/discrete reaction field spectra of open shell systems: The visual spectrum of $[\text{Fe}^{\text{III}}(\text{PyPepS})_2]^-$ in aqueous solution

Piet Th. van Duijnen,^{a)} Shannon N. Greene, and Nigel G. J. Richards

Department of Chemistry, University of Florida, Gainesville, Florida 32611-7200

and Quantum Theory Project, University of Florida, Gainesville, Florida 32611-7200

(Received 12 February 2007; accepted 29 May 2007; published online 31 July 2007)

We report the calculated visible spectrum of $[\text{Fe}^{\text{III}}(\text{PyPepS})_2]^-$ in aqueous solution. From all-classical molecular dynamics simulations on the solute and 200 water molecules with a polarizable force field, 25 solute/solvent configurations were chosen at random from a 50 ps production run and subjected the systems to calculations using time-dependent density functional theory (TD-DFT) for the solute, combined with a solvation model in which the water molecules carry charges and polarizabilities. In each calculation the first 60 excited states were collected in order to span the experimental spectrum. Since the solute has a doublet ground state several excitations to states are of type “three electrons in three orbitals,” each of which gives rise to a manifold of a quartet and two doublet states which cannot properly be represented by single Slater determinants. We applied a tentative scheme to analyze this type of spin contamination in terms of Δ and Δ transitions between the same orbital pairs. Assuming the associated states as pure single determinants obtained from restricted calculations, we construct conformation state functions (CFSs), i.e., eigenfunctions of the Hamiltonian \hat{S}_z and \hat{S}^2 , for the two doublets and the quartet for each Δ , Δ pair, the necessary parameters coming from regular and spin-flip calculations. It appears that the lower final states remain where they were originally calculated, while the higher states move up by some tenths of an eV. In this case filtering out these higher states gives a spectrum that compares very well with experiment, but nevertheless we suggest investigating a possible (re)formulation of TD-DFT in terms of CFSs rather than determinants. © 2007 American Institute of Physics. [DOI: 10.1063/1.2751164]

INTRODUCTION

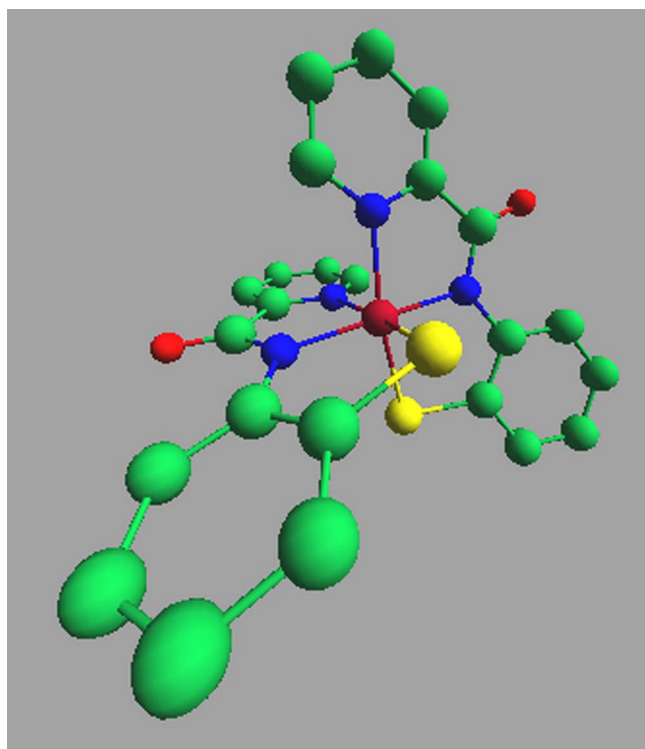
$[\text{Fe}^{\text{III}}(\text{PyPepS})_2]^-$ (Fig. 1) is a chemical model for the active site of Fe-dependent nitrile-hydratase (NHase), a non-heme Fe(III) enzyme that catalyzes the hydration of nitriles to amides.¹ It was first synthesized and characterized by Noveron *et al.*² The native enzyme and $[\text{Fe}^{\text{III}}(\text{PyPepS})_2]^-$ have characteristic (visible) spectra (see Fig. 2) showing strong absorption in the 400–500 nm region and a weaker band around 700–800 nm.³

We report a computational study on the visible spectrum of $[\text{Fe}^{\text{III}}(\text{PyPepS})_2]^-$ in aqueous solution in order to find out whether time-dependent density functional theory/molecular mechanics (TD)DFT/MM is able to describe the properties of the complex and the parent enzyme, the spectra being a good test. Several computational studies were devoted to NHase and its active site models. Boone *et al.*⁴ conducted DFT calculations on various models, among which is $[\text{Fe}^{\text{III}}(\text{PyPepS})_2]^-$, establishing that it has a doublet ground state both in the gas phase and in aqueous solution. Greene and Richards⁵ report calculations on models based on the actual x-ray structure of the enzyme. They address the spin

states of the various models and give their UV-visible spectra as calculated with the semiempirical INDO/S CIS method.⁶ The spectra are very similar to that in Fig. 2 with relatively large oscillator strength near 300–500 nm and a weaker but clear band in the 600–900 nm region.

Efforts to calculate the spectrum of $[\text{Fe}^{\text{III}}(\text{PyPepS})_2]^-$ in solution with the same approach, i.e., a combination of (TD)DFT/MM (geometry optimization of the complex surrounded by 50 water molecules, followed by INDO/S CIS after which the whole sample after equilibration was treated quantum mechanically), failed for several reasons.⁷ INDO is a minimum basis approach which is unable to describe negative ions properly: in the analysis of the charge distribution of the resulting SCF wave function all water molecules were slightly negative to an extent that the complex “lost” about two electrons, and, hence the calculated spectrum belonged to $[\text{Fe}^{\text{III}}(\text{PyPepS})_2]^+$ rather than to the negative ion itself. Moreover, 50 water molecules are insufficient to make up even the first solvation shell of $[\text{Fe}^{\text{III}}(\text{PyPepS})_2]^-$ and it appeared that the water molecules were unrealistically close to the solute. Therefore we turned to the discrete reaction field (DRF) approach^{8,9} which was implemented in INDO (Ref. 10) within the Rumer-CI scheme.¹¹ In DRF the solvent is modeled classically, thus avoiding the “charge transfer” problem, while still treating the many-body polarization self-consistently like in a full SCF calculation.^{12,13} We took a

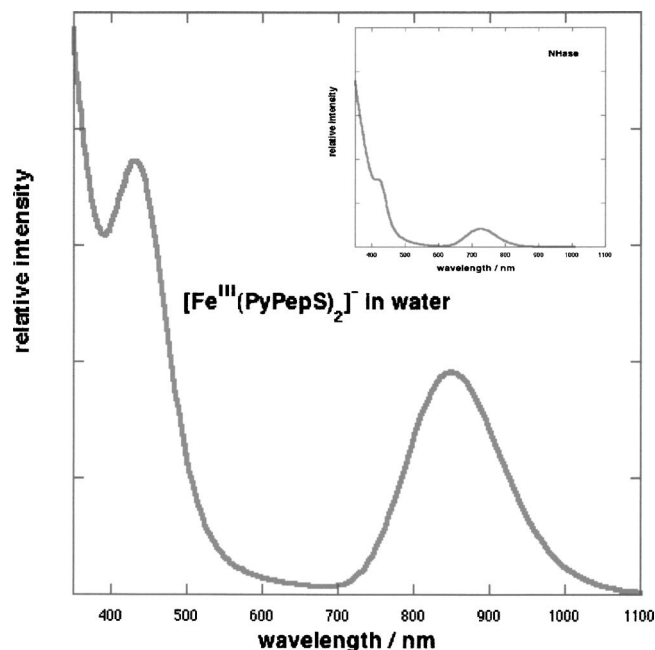
^{a)}Author to whom correspondence should be addressed. Permanent address: Theoretical Chemistry, Zernike Institute for Advanced Materials, Rijksuniversiteit, Nijenborgh 4, 9747 AG Groningen, The Netherlands. Electronic mail: p.t.van.duijnen@rug.nl

FIG. 1. (Color online) Perspective view of $\text{Fe}(\text{PyPepS})_2$.

sequential approach in which one first performs a classical simulation on the system and saving, after equilibration, a number of snapshots that are subject to completely quantum mechanical or quantum mechanical/molecular mechanics QM/MM calculations. The number of (uncorrelated) snapshots, needed in order to obtain statistically significant results, is very small in comparison with the number of time steps in, e.g., a molecular dynamics simulation.¹⁴ For the required MD simulations we applied the DRF90 program,¹⁵ i.e., the all-classical form of DRF, on $[\text{Fe}^{\text{III}}(\text{PyPepS})_2]^-$ in 200 water molecules. This gave normal solute/solvent distances and two solvation shells. From the MD simulations we obtained 100 solute/solvent configurations from which “solvated” INDO spectra were calculated. All showed relatively large oscillator strength in the 300–400 nm region but were virtually empty beyond 500 nm. The gas phase spectrum had a very weak band at 870 nm that was not present in solution. This is probably caused by the combination of a charged species in solution with a minimal basis.

Next we moved to TD-DFT. We used the Amsterdam density functional (ADF) package,¹⁶ in which DRF is also implemented,⁹ again using 200 water molecules. The calculated spectrum is very similar to the experimental one but in comparison slightly redshifted. The shift could be due to the fact that $[\text{Fe}^{\text{III}}(\text{PyPepS})_2]^-$ has an open shell ground state, which is problematic in TD-DFT and possibly leads to systematic errors.

In the following sections we briefly summarize the DRF approach, discuss the fundamental problem with calculations of spectra of open shell systems with TD-DFT and a tentative effort to analyze this problem. We give gas phase and solvated spectra and compare them with experiment. Finally, we present some conclusions.

FIG. 2. Experimental spectra of $[\text{Fe}^{\text{III}}(\text{PyPepS})_2]^-$ and (inset) of NHase in water.

THE DISCRETE REACTION FIELD (DRF) APPROACH

In the DRF approach^{8,9,17} a solute is described by any QM method (the QM system), whereas the solvent is modeled with MM by any number of discrete molecules and, optionally, an enveloping dielectric continuum (extending the MM system). The permanent charge distribution of a solvent molecule is represented by point charges, mainly at the constituent atoms, but more sites may be used to represent moments beyond the dipole moment. The charges needed are obtained from appropriate quantum chemical calculations.^{18,19} Changes in the charge distribution, due to interactions with other parts of the system, are taken care of by polarizabilities located either at the atoms (distributed polarizability model) or at appropriate centers (group polarizability model). Polarizabilities are obtained from appropriate quantum chemical calculations or from fitting to experimental results.^{20–22}

Thus, the (effective) Hamiltonian of the complete system is written as

$$\hat{H} = \hat{H}_{\text{QM}} + \hat{H}_{\text{QM/MM}} + \hat{H}_{\text{MM}}, \quad (1)$$

with \hat{H}_{QM} the solute's quantum mechanical Hamiltonian, \hat{H}_{MM} the classical Hamiltonian of the classical solvent, while $\hat{H}_{\text{QM/MM}}$ describes the solute/solvent interactions. Within the DRF approach the QM/MM operator at a point r_i is generally given by

$$\hat{H}_{\text{QM/MM}}(r_i) = \hat{\nu}^{\text{DRF}}(r_i) = \hat{\nu}^{\text{es}}(r_i) + \hat{\nu}^{\text{pol}}(r_i) + \hat{\nu}^{\text{rep}}(r_i), \quad (2)$$

with $\hat{\nu}^{\text{es}}(r_i)$ the electrostatic operator describing the Coulombic interaction between the QM solute and the static charge distribution of the MM solvent, $\hat{\nu}^{\text{pol}}(r_i)$ the polarization operator describing the many-body polarization of the solvent molecules, i.e., the changes in the charge distribution of these molecules due to interactions with the QM solute and

other parts of the MM solvent, and $v^{\text{rep}}(r_i)$ the (model) Pauli repulsion term that is only important for molecular dynamics (MD) as it does not affect the electrons.

Because the solvent charge distribution is represented by point charges, the electrostatic operator is simply

$$\hat{v}^{\text{es}}(r_i) = \sum_s \frac{q_s}{R_{si}} = \sum_s q_s T_{si}^{(0)}, \quad (3)$$

where the index s runs over all charged sites in the solvent, and we introduced the zeroth-order tensor. The general form of the interaction tensors to a given order n is

$$T_{pq, \alpha_1, \dots, \alpha_n}^{(n)} = \nabla_{pq, \alpha_1} \dots \nabla_{pq, \alpha_n} \left(\frac{1}{R_{pq}} \right), \quad (4)$$

with R_{pq} the distance between sites p and q . We note that if the solute is represented too by point charges and polarizabilities, Eqs. (1) and (2) define a classical polarizable force field. The degrees of freedom of the solution are sampled by MD using DRF90¹⁵. For details of QM/MM see, for example, van Duijnen and de Vries^{8,23} or Jensen and van Duijnen.¹³

TD-DFT SPECTRA FROM A DOUBLET GROUND STATE

From a doublet ground state three types of spin allowed single electron excitation are possible:

- (I) from the (singly occupied) highest occupied molecular orbital (HOMO) to unoccupied molecular orbitals (MOs),
- (II) from any doubly occupied MO to the (singly occupied) HOMO,
- (III) from any doubly occupied MO to unoccupied MOs.

Since TD-DFT is essentially a one-determinant approach, excited states resulting from types I and II transitions can represent proper spectroscopic states in the sense that they are approximations to eigenfunctions of both the Hamiltonian and the spin operators \hat{S}_z and \hat{S}^2 . However, excitations of type III give states, as single determinants, which are eigenfunctions of \hat{S}_z only. Using d for any doubly occupied orbital, s for the singly occupied orbital, and a for any unoccupied orbital (in the ground state), the type III determinants are of the form $|\bar{d}sa\rangle$ and $|dsa\rangle$, respectively, assuming that s was originally an α spinorbital and that the bar indicates a β spinorbital. They are part of the manifold associated with the “three electrons in three orbitals” configurations, i.e., the eight determinants spanning a representation of a quartet and two doublet states.

From the determinants:

$$d_1 = |\bar{d}sa\rangle, \quad d_2 = |\bar{d}sa\rangle, \quad d_3 = |dsa\rangle, \quad d_4 = |dsa\rangle, \quad (5)$$

the following proper configuration state functions (CFs) with $M_s = 1/2$ can be constructed:

$$D_1 = \frac{1}{\sqrt{6}}\{2d_1 - d_2 - d_3\}, \quad D_2 = \frac{1}{\sqrt{2}}\{d_2 - d_3\}, \quad (6)$$

$$Q_1 = \frac{1}{\sqrt{3}}\{d_1 + d_2 + d_3\}.$$

Assuming that α and β spinorbitals have the same spatial parts, and defining the determinantal energies as $e_{ii} = \langle d_i | \hat{H} | d_i \rangle$ we get

$$e_{11} = C + J - K_{da},$$

$$e_{22} = C + J - K_{sa},$$

$$e_{33} = C + J - K_{ds},$$

$$e_{44} = C + J - (K_{ds} + K_{sa} + K_{da}),$$

with C the one-electron and J the two-electron Coulomb energy, respectively, common to all determinants, and the K 's the appropriate exchange energies. For the state energies we obtain

$$E(D_1) = \frac{1}{6}\{4e_{11} + e_{22} + e_{33} + 4(K_{ds} + K_{sa}) - 2K_{da}\},$$

$$E(D_2) = \frac{1}{2}\{e_{22} + e_{33} - 2K_{da}\},$$

$$E(Q) = \frac{1}{3}\{e_{22} + e_{22} + e_{33}\} = e_{44}. \quad (8)$$

We note that D_1 and D_2 are orthogonal but not unique and there may be a nonzero interaction matrix element between them,

$$k_{12} = \langle D_1 | \hat{H} | D_2 \rangle = \frac{3}{\sqrt{12}}\{K_{sa} - K_{ds}\}. \quad (9)$$

From the following equalities:

$$e_{11} - e_{22} = K_{sa} - K_{da},$$

$$e_{22} - e_{33} = K_{ds} - K_{sa},$$

$$e_{11} - e_{44} = K_{ds} + K_{sa}, \quad (10)$$

the three K 's can be evaluated and, hence, the two doublet CSF energies and the interaction matrix element, provided all e_{ii} are known. The final doublets states are then obtained from the simple secular equation

$$\begin{vmatrix} E(D_1) - \varepsilon & k_{12} \\ k_{12} & E(D_2) - \varepsilon \end{vmatrix} = 0. \quad (11)$$

In this case, e_{22} and e_{33} are the excitations obtained from a normal calculation of the spectrum, while e_{11} and e_{44} come from a “spin-flip” calculation where an electron excited from a Δ spin orbital is put into a Δ spin orbital or vice versa. In fact, from the ground state $|\bar{d}ds\rangle$ the spin-flip produces $|\bar{d}sa\rangle$ instead of $|\bar{d}sa\rangle$ and $|\bar{d}sa\rangle$ instead of $|\bar{d}sa\rangle$ but the energies of these pairs are the same under our assumptions.

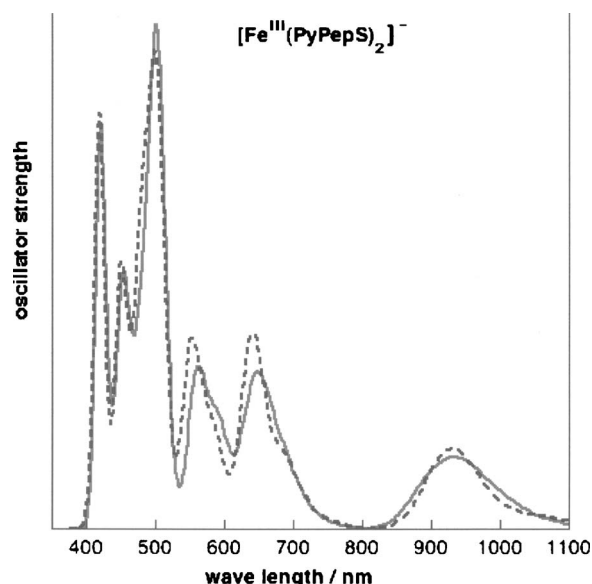


FIG. 3. Gas phase spectrum from TZP (solid line) and DZ (dashed line) basis sets. Individual excitations broadened with Gaussians with a bandwidth of 0.14 eV.

COMPUTATIONAL DETAILS

First we calculated the spectrum of $[\text{Fe}^{\text{III}}(\text{PyPepS})_2]^-$ in the gas phase applying TD-DFT as implemented in the RESPONSE module of ADF using the DZ and the TZP default Slater basis sets using a statistical average of orbital model exchange-correlation potential (SAOP)²⁴. In order to span the width of the experimental spectrum in aqueous solution the 60 lowest excited states were calculated. The resulting spectra, broadened by Gaussians with a bandwidth of 0.005 h, are displayed in Fig. 3, showing that they are so similar that we decided, for reasons of efficiency, to use the DZ basis for the DRF/QM/MM calculations.

Classical MD simulations were performed on $[\text{Fe}^{\text{III}}(\text{PyPepS})_2]^-$ immersed in 200 water molecules using the DRF90 program¹⁵ with rigid solute and solvent molecules and a time step of 1 fs at a temperature of 298 K, controlled by a Nose-Hoover thermostat²⁵ in an NVT ensemble. We used only one solute conformation because other conformations of the complex are not very likely. The solute's geometry was taken from Ref. 26 while the atomic charges generating the molecular field up to the quadrupole moment¹⁹ came from the vacuum ground state calculation. The charges on the atoms of a water molecule are such that they give the experimental dipole moment. Other parameters are the DRF90 defaults,¹⁵ except for Fe for which we took a polarizability of 40 a.u. The molecules were placed in a (virtual) sphere with a radius of 23.6 bohr, and a soft wall force¹⁵ was applied to keep the molecules from evaporating. Equilibration runs of at least 20 ps were performed, followed by 50 ps production runs from which 100 uncorrelated solute/solvent configurations were selected and saved. The saved solute/solvent configurations were used in TD-DFT/DRF runs to calculate the energies of the 60 lowest energy electronic states and the corresponding oscillator strengths. Usually we take 50–100 solute/solvent configurations for the QM/MM calculations, but since SAOP is only applicable in all-electron calculations

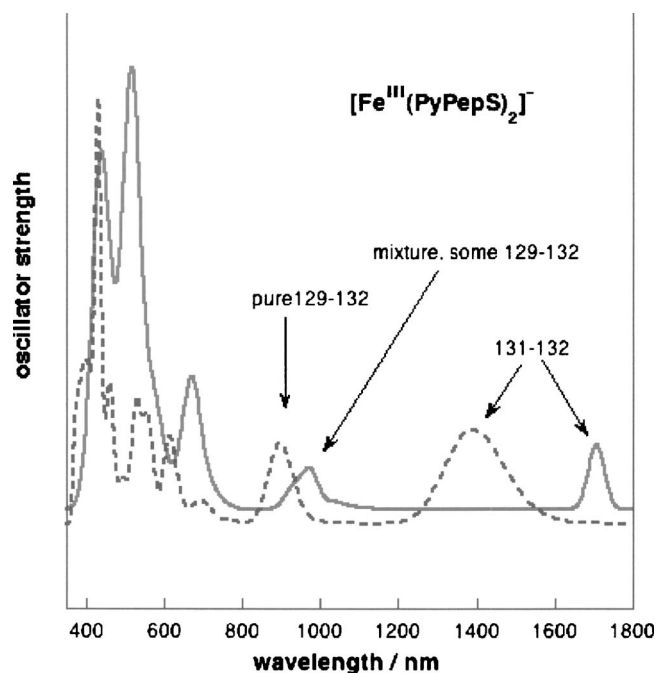


FIG. 4. Spectrum of a single solute/solvent configuration (dashed line) compared with the gas phase spectrum (drawn line). Normalized spectra, broadened by gaussians with a bandwidth of 0.14 eV.

we took only 25 configurations, after checking with less expensive methods that the spectra from 25 and 50 configurations are virtually the same. Jensen *et al.*²⁷ argue that solvent effects on spectra are mainly due to the solvation of the ground state, and that spectra of highly charged systems in polar molecules are hardly affected by dynamic polarization of the solvent. Although the present system is not highly charged, test calculations also revealed that in this case the dynamic solvent response—which requires evaluation of densities and induced dipoles for each excited state in each iteration of the diagonalization of the TD-DFT matrix—can be neglected, which also leads to a significant reduction in computer time.

RESULTS AND DISCUSSION

In Fig. 4 we compare the gas phase spectrum with that of a single solute/solvent configuration. Each single vertical transition has been broadened with a Gaussian with a bandwidth of 0.14 eV to mimic the internal vibrations. The numbers point at the contributions of the bands in terms of orbital transitions.

We note a blueshift going from the gas phase to the condensed phase. This is to be expected since the excited states will not be in equilibrium with the solvent, which was equilibrated with the ground state's charge distribution.

The computed (solvated) spectrum shows all the features of the experimental spectrum, i.e., high intensity in the 300–600 nm region, a weak band around 900 nm and, beyond the visible region, a band at 1500 nm. The computed visible spectrum appears to be redshifted by some 50 nm.

Therefore we looked into a possible systematic error due to the use of TD-DFT for computing spectra of systems with doublet ground states. These calculations are done as spin

TABLE I. Correction table for (α, β) and (β, α) excitations present in both the normal calculation and in the spin-flip calculation. Single solute/solvent configuration. For explanation of symbols, see text.

States	Orbitals involved	e_{11}	K_{ds}	E_1	D_1	Δ_1
		e_{22}	K_{sa}	E_2	D_2	Δ_2
4	$131 \rightarrow 133$	e_{33}	K_{da}	k_{12}		
		e_{44}				
6	$131 \rightarrow 133$	1.78	0.19	1.90	1.97	0.20
		1.76	0.04	1.67	1.61	0.00
		1.61	0.02	0.02		
5	$131 \rightarrow 134$	1.55				
		1.89	0.24	2.02	2.13	0.18
		1.95	0.01	1.77	1.66	-0.06
9	$131 \rightarrow 134$	1.72	0.06	0.04		
		1.65				
		2.48	0.41	2.70	2.88	0.38
11	$129 \rightarrow 133$	2.50	0.03	2.26	2.08	-0.03
		2.21	0.05	0.11		
		2.05				
13	$130 \rightarrow 134$	2.57	0.45	2.81	3.00	0.41
		2.58	0.04	2.32	2.14	-0.03
		2.17	0.05	0.13		
27	$131 \rightarrow 135$	2.08				
		2.58	0.30	2.87	2.87	0.52
		2.34	0.30	2.28	2.28	-0.06
17	$131 \rightarrow 135$	2.35	0.07	0.00		
		1.98				
		2.68	0.18	2.83	2.84	0.28
19	$131 \rightarrow 136$	2.56	0.14	2.52	2.51	-0.01
		2.52	0.02	0.00		
		2.36				
22	$128 \rightarrow 134$	3.14	0.44	3.39	3.55	0.40
		3.15	0.07	2.88	2.73	-0.05
		2.78	0.08	0.10		
49	$131 \rightarrow 138$	2.62				
		3.19	0.54	3.57	3.66	0.62
		3.05	0.22	2.81	2.72	-0.05
34	$131 \rightarrow 138$	2.73	0.06	0.08		
		2.43				
		3.26	0.15	3.40	3.40	0.22
44	$127 \rightarrow 134$	3.19	0.13	3.12	3.12	-0.05
		3.17	0.06	0.00		
		2.97				

unrestricted, i.e., leading to different orbitals for different spins. The expectation value of \hat{S}^2 for the ground state was 0.78 where it should be 0.75. A ground state calculation of the lowest quartet gave $\langle \hat{S}^2 \rangle = 3.86$ while it should be 3.75. These numbers indicate that the amount of spin contamination due to the unrestricted character of the calculation is not too serious. $[\text{Fe}^{\text{III}}(\text{PyPepS})_2]^-$ has 263 electrons and hence 131 doubly occupied MOs and one singly occupied HOMO(132). This makes $131 \rightarrow 133$ the first “type III” transition. Fortunately this transition of a β electron is present—in a typical “solvated” spectrum for an arbitrary single solute/solvent configuration—with a weight of about 90% in the final state at about 1.61 eV (e_{33}). It is accompanied by nearly degenerate α transitions at (averaged) 1.76 eV

(e_{22}) with a combined weight of about 80%. From the spin-flip calculation we found the quartet at 1.55 eV (e_{44}) and the $M_s = 1/2$ term at 1.78 eV (e_{11}). The quartet ground state energy from a normal calculation differs less than 0.01 eV from the spin-flip result e_{44} , showing the internal consistency of the calculations. Putting these numbers into Eq. (10) we arrive at $E(D_1) = 1.90$ and $E(D_2) = 1.67$ eV with an interaction matrix element of 0.02 eV. From solving Eq. (11) we find final states at 1.97 and 1.61 eV, i.e., shifts of 0.18 (~ 70 nm) and 0.00 eV, respectively, from the state energies. In Table I results for all Δ, Δ combinations, present in both the regular and the spin-flip transitions, are collected. The conclusion so far is that the lower final states hardly move, while the higher states move up to some tenths of an eV

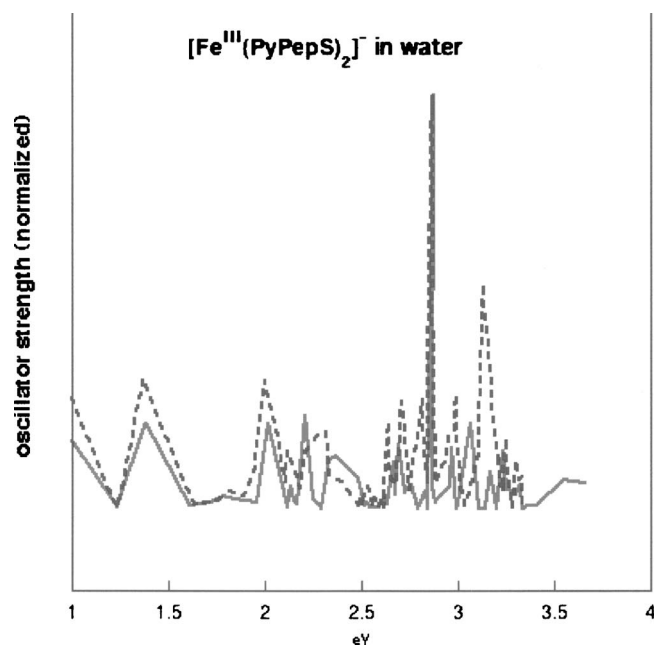


FIG. 5. Comparison between uncorrected (solid line) and corrected (dashed line) spectrum for a single solute configuration.

upwards, with a tendency to larger differences for higher lying states. Using the contents of Table I one could try to correct the spectra but one must realize that only nine cases could be found—out of the 60 transitions—to be used in this scheme because the remaining transitions are either not of type III, lack partners in the range of excitations calculated, or are not matched in the spin-flip results. Unmatched transitions in the regular spectrum are the lower energy partners of possible α, β pairs that move little. This is encouraging since the first few excited states are related to types I and II transitions which are unaffected, as are the lower energies of the pairs. Treating all solute/solvent configurations in this way is awkward and (computer) time consuming since it would at least double the effort, due to the required spin-flip calculations. Moreover, all this is very approximate of course, because the states are no pure determinants, and the α and β orbitals are different in the present unrestricted treatment. Therefore the best approach here is probably keeping the lower states of pairs and unpaired type III states as they are and filter out the higher lying partners of pairs by assigning zero oscillator strength to them. This is fairly simple and at least eliminates spurious energies. Results are in Fig. 5, from which we learn that the spectrum will change only slightly. Other cases may turn out differently and it is probably worthwhile to investigate a reformulation of TD-DFT in a restricted treatment²⁸ in terms of CFSs rather than determinants, much alike the singlet-triplet calculations on closed-shell ground states.²⁹ This is, however, beyond the scope of this paper.

Other TD-DFT studies on spectra from doublet ground states show differences with experiment (averaged over several molecules) typically of about 0.2 eV for some small molecules in the gas phase showing only types I and II excitations,³⁰ and about 0.3–0.4 eV if gas phase calculations are compared with condensed phase experiments.^{28,31} Even

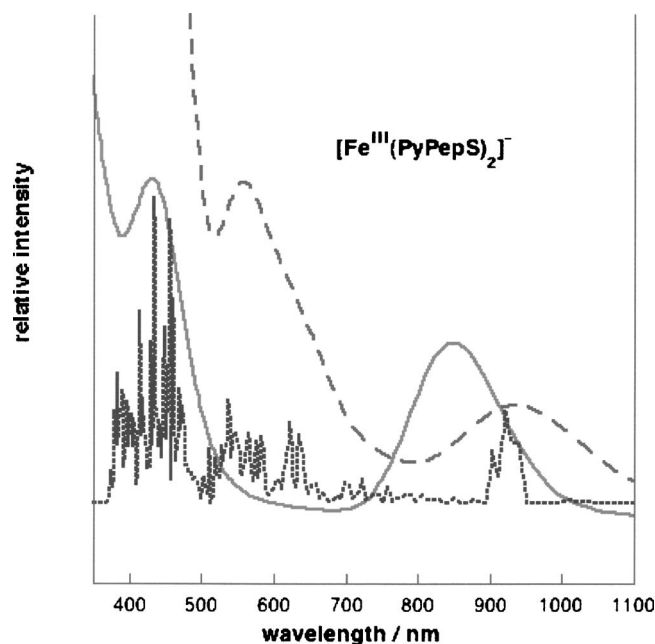


FIG. 6. Experimental visible spectrum (solid line) reconstructed from Ref. 2 with three Gaussians. Computed spectrum (dashed line) of 25 solute/solvent configurations collected in 60 boxes and broadened with Gaussians with bandwidth of ~ 0.3 eV, and (dotted) the same, collected in 200 boxes without broadening.

calculations of spectra of molecules with closed-shell ground states give similar differences.²⁹ This is to our knowledge the first time that an experimental spectrum of an open shell system in solution can be compared with a DFT calculation under similar conditions. This may raise the question whether the present solvation model is responsible for differences between the calculated and the experimental spectra. Totally classical calculations with DRF90 have been shown to be in perfect agreement with both accurate QM calculations and experiment.^{12,15,23} Spectra calculated with DRF, based on *ab initio* wave functions,³² semiempirical,³³ or DFT,⁹ compared reasonably well with experiment. Hence we are confident that the interaction energies are in general better than the margins just discussed.

Our final “filtered” results are given in Fig. 6, for which the oscillator strengths from the 25 solute/solvent configurations were collected in 200 equal energy boxes, i.e., with box widths of ~ 7 nm. The structure of the bands appearing at this resolution are due to the thermal movements of the solvent molecules around the rigid solute. By collecting the data in 60 boxes and by applying Gaussians with a bandwidth of ~ 0.3 eV, we mimicked “missing” structural changes of the solute, possibly present in the experiments, and we obtain a spectrum with a resolution comparable with the experimental spectrum, also presented in Fig. 6. We conclude that the computed spectrum is quite acceptable with its 0.11 eV shift of the band at about 900 nm. Differences in the 400–600 nm region are about 0.6 eV if the shoulder computed at 550 nm should be associated with the 440 nm shoulder of the experimental spectrum. The bands at 700–900 nm in various model compounds are usually regarded as $S \rightarrow Fe$ charge transfer transitions.^{1,5,34} In Fig. 7 the MOs related to the (far) infrared bands are depicted. From them and Table II we con-

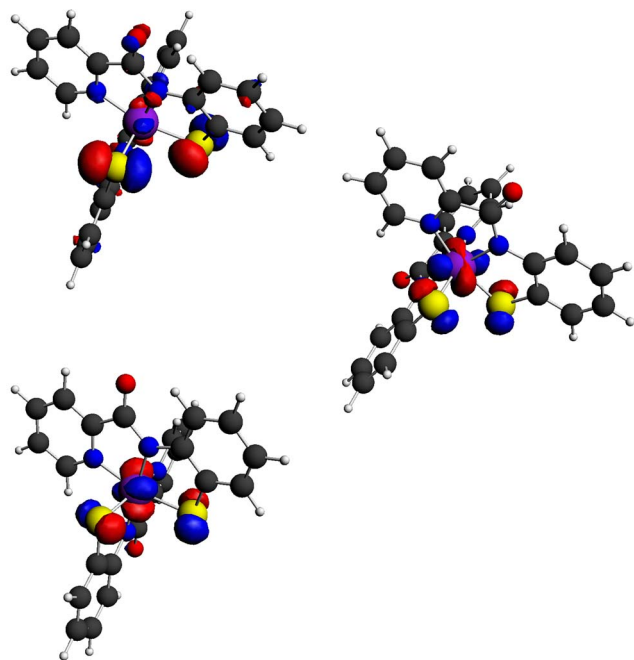


FIG. 7. (Color online) Molecular orbitals 129, 131, and 132 of $[\text{Fe}^{\text{III}}(\text{PyPepS})_2]^-$ in water.

clude that the $129 \rightarrow 132$ band at ~ 920 nm is a $d_\pi \rightarrow d_\pi$ transition (found by Greene and Richards⁵ at ~ 2000 nm for a different model compound) and the $131 \rightarrow 132$ band at ~ 1500 nm the $\text{S} \rightarrow \text{Fe}$ charge transfer transition. The differences between the assignments here and in Ref. 5 and others may be related to the differences in the systems studied.

We followed the suggestion of a referee and looked into the effect of possible hydrogen bonding on the spectrum. Kovacs¹ discussed a blueshift of the ~ 700 nm bands going from an aprotic solvent to water for a number of model compounds. More specifically, for $[\text{Fe}^{\text{III}}(\text{DITpy})_2]^+$ the 784 nm band in MeCN shifts to 732 nm in water, and it was suggested that this is a consequence of the “increased H-bonding ability” of the latter solvent. In Fig. 8 we present the radial distribution of water with respect to S1 or S2 constructed from 100 solute/solvent configurations. It shows that, on av-

TABLE II. Major contributions of basis functions to the β MOs involved in the (far) infrared transitions.

MO	%	Basis function	Atom
129	34	d_{xy}	Fe
	23	d_{yz}	Fe
	11	p_x	S ₁
	8	p_z	S ₂
131	22	p_z	S ₂
	21	p_x	S ₁
	9	d_{xy}	Fe
132	44	d_{xz}	Fe
	11	p_x	S ₁
	8	p_z	S ₂
	8	d_{yz}	Fe

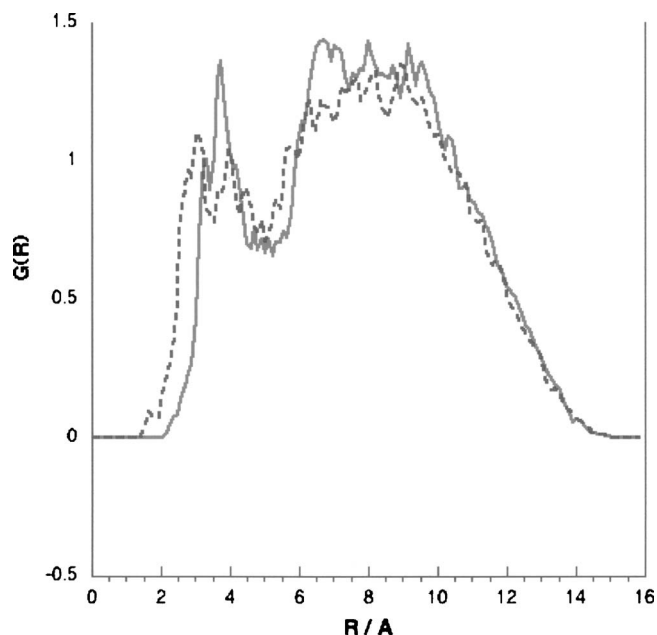


FIG. 8. Radial distributions of O (water, solid line) and H (water, dashed line) relative to S of $[\text{Fe}^{\text{III}}(\text{PyPepS})_2]^-$ obtained from 100 solute/solvent configurations.

erage, there is indeed about one water molecule that might be “hydrogen bonded” to S although at the much too large O–S distance of 3.5 Å. Other candidates for hydrogen bonding, i.e., the oxygens, are ruled out for the same reason, the O–O distance being about 3.4 Å. Nevertheless we reconstructed a situation with $[\text{Fe}(\text{PyPepS})_2]^-$ and a single water molecule “hydrogen bonded” at one of the sulfur atoms at the distance of Fig. 7, and calculated the spectrum fully quantum mechanically. As expected, the spectrum obtained was identical to the gas phase spectrum. On optimizing the “hydrogen bond” the water molecule was actually expelled, which is not surprising in the light of the positive Mulliken³⁵ and Voronoi³⁶ charges on the sulfur atoms of about 0.2. From this we conclude that this water molecule is put and kept there by the hydrogen bond network of the solvent and that the blueshift of the solvated spectrum with respect to the gas phase (see Fig. 4) is induced by the bulk of the solvent and not by specific interactions like hydrogen bonding. The spectrum of $[\text{Fe}(\text{PyPepS})_2]^-$ in dimethyl sulfoxide³ (DMSO) has a 878 nm band while it is in water at 850 nm. This shift can easily be explained in terms of the different packing of the two solvents: putting 200 DMSO molecules around the solvent requires about six times the volume needed for 200 waters and although the ratio between the dipole moments of DMSO (6.43 D) and water (1.88 D) is 3.4, the dipole density in water is much larger which interacts with the solute at smaller distances.

CONCLUSIONS

We present the first successful calculation of the visible spectrum of $[\text{Fe}^{\text{III}}(\text{PyPepS})_2]^-$ —a model active site of Fe-dependent N-hydratase—in aqueous solution, using the TDDFT modules of ADF for the quantum mechanical treatment of the solute with the DRF approach for the solute/solvent

interactions. For each of 25 solute/solvent configurations, obtained from MD simulations with the polarizable force field of the DRF90 program, the 60 lowest excited states were calculated and collected into a single spectrum. The resulting spectrum is very close to the experimental and it is blue-shifted in comparison with the gas phase. We found no hydrogen bonds with the solute in the structures and attribute this shift solely to effect of bulk solvent. The calculated spectrum is somewhat redshifted with respect to experiment. We investigated whether this was caused by the formal error made in TD-DFT by representing excited states with single determinants where linear combinations are needed to arrive at eigenfunctions of both \hat{S}_z and \hat{S}^2 . However, possible corrections are within the margins usually found in TD-DFT spectra and we conclude that the presently calculated spectrum is trustworthy for the long wavelength part, but may be in error by 0.5 eV in the near UV edge. We suggest investigating the possibility of reformulating TD-DFT in terms of a many determinant approach for spectra of systems with open shell ground states, in particular for the high-energy parts of spectra. This study was started to see whether our approach, i.e., the sequential TD-DFT/MM approach where classical MD simulations are used to generate solute/solvent configurations, followed by QM/MM calculations to arrive at electronic properties of the system in solution, is good enough to treat (parts of) an enzyme similarly. In that sense the present result shows that this is possible even in the present implementation of DRF/TD-DFT and we will treat native NHase similarly.

ACKNOWLEDGMENTS

One of the authors (P.T.v.D.) thanks M.E. Casida (Grenoble) for a stimulating discussion and R. Broer (Groningen) for help with the matrix elements. The authors thank the National Science Foundation (CHE-0079008) for their support (P.T.v.D. and S.N.G.).

¹J. A. Kovacs, Chem. Rev. (Washington, D.C.) **104**, 825 (2004).

²J. C. Noveron, M. M. Olmstead, and P. K. Mascharak, Inorg. Chem. **37**, 1138 (1998).

³L. A. Tyler, J. C. Noveron, M. M. Olmstead, and P. K. Mascharak, Inorg. Chem. **38**, 616 (1999).

⁴A. M. Boone, C. H. Chang, S. N. Greene, T. Herz, and N. G. J. Richards,

Coord. Chem. Rev. **238-239**, 291 (2003).

⁵S. N. Greene and N. G. J. Richards, Inorg. Chem. **45**, 17 (2006).

⁶M. C. Zerner, in *Reviews of Computational Chemistry*, edited by K. B. Lipkowitz and D. B. Boyd (VCH, New York, 1991), Vol. 2, p. 313.

⁷S. N. Greene and P. Th. van Duijnen (unpublished).

⁸A. H. de Vries, P. Th. van Duijnen, A. H. Juffer, J. A. C. Rullmann, J. P. Dijkman, H. Merenga, and B. T. Thole, J. Comput. Chem. **16**, 37 (1995).

⁹L. Jensen, P. Th. van Duijnen, and J. G. Snijders, J. Chem. Phys. **118**, 514 (2003).

¹⁰P. Th. van Duijnen (unpublished).

¹¹R. Manne and M. C. Zerner, Int. J. Quantum Chem., Quantum Chem. Symp. **19**, 165 (1986).

¹²F. Grozema, R. W. J. Zijlstra, and P. Th. van Duijnen, Chem. Phys. **246**, 217 (1999).

¹³L. Jensen and P. Th. van Duijnen, in *Atoms, Molecules and Clusters in Electric Fields; Theoretical Approaches to the Calculation of Electric Polarizability*, edited by G. Maroulis (Imperial College Press, London, 2006).

¹⁴K. Coutinho, M. J. D. Oliveira, and S. Canuto, Int. J. Quantum Chem. **66**, 249 (1998).

¹⁵M. Swart and P. Th. van Duijnen, Mol. Simul. **32**, 471 (2006).

¹⁶SCM, Amsterdam density functional theory (URL <http://www.scm.com>, Amsterdam).

¹⁷B. T. Thole and P. Th. van Duijnen, Theor. Chim. Acta **55**, 307 (1980).

¹⁸B. T. Thole and P. Th. van Duijnen, Theor. Chim. Acta **63**, 209 (1983).

¹⁹M. Swart, P. Th. van Duijnen, and J. G. Snijders, J. Comput. Chem. **22**, 79 (2001).

²⁰B. T. Thole, Chem. Phys. **59**, 341 (1981).

²¹P. Th. van Duijnen and M. Swart, J. Phys. Chem. A **102**, 2399 (1997).

²²M. Swart, P. Th. van Duijnen, and J. G. Snijders, J. Mol. Struct.: THEOCHEM **458**, 11 (1999).

²³P. Th. van Duijnen and A. H. de Vries, Int. J. Quantum Chem. **60**, 1111 (1996).

²⁴P. R. T. Schipper, O. V. Gritsenko, S. J. A. van Gisbergen, and E. J. Baerends, J. Chem. Phys. **112**, 1344 (2000).

²⁵T. Toxvaerd, Mol. Phys. **72**, 159 (1972).

²⁶S. N. Greene, C. H. Chang, and N. G. Richards, Chem. Commun. (Cambridge) **2002**, 2386.

²⁷L. Jensen, M. Swart, P. Th. van Duijnen, and J. Autschbach, Int. J. Quantum Chem. **106**, 2479 (2006).

²⁸Z. Rinkevicius, I. Tunell, P. Salek, O. Vahtras, and H. Ågren, J. Chem. Phys. **119**, 34 (2003).

²⁹S. J. A. van Gisbergen, J. G. Snijders, and E. J. Baerends, Comput. Phys. Commun. **118**, 119 (1999).

³⁰S. Hirata and M. Head-Gordon, Chem. Phys. Lett. **314**, 291 (1999).

³¹F. Wang and T. Ziegler, Mol. Phys. **102**, 2585 (2004).

³²F. Grozema and P. Th. van Duijnen, J. Phys. Chem. A **102**, 7984 (1998).

³³P. Th. van Duijnen and T. L. Netzel, J. Phys. Chem. A **110**, 2204 (2006).

³⁴H. L. Jackson, S. C. Shoner, D. Rittenberg, J. A. Cowen, S. Lovell, D. Barnhart, and J. A. Kovacs, Inorg. Chem. **40**, 1646 (2001).

³⁵R. S. Mulliken, J. Chem. Phys. **23**, 1841 (1955).

³⁶C. Fonseca Guerra, J.-W. Handgraaf, E. J. Baerends, and F. M. Bickelhaupt, J. Comput. Chem. **25**, 189 (2004).